Analysis on the refrigerant (R32) flow maldistribution of microchannel heat exchanger under superheat and sub-cool

M. H. Chng[1,2]*, W. M. Chin[2] and S. H. Tang[1]

[1]Faculty of Engineering, Universiti Putra Malaysia, 43400 UPM Serdang,
Selangor Darul Ehsan. Malaysia
*Email: chngminghui88@gmail.com
Phone: +60122310614
[2]Daikin R&D Centre Sdn Bhd, Lot 60334, Persiaran Bukit Rahman Putra 3, Taman
Perindustrian Bukit Raman Putra, 47000 Sungai Buloh, Selangor, Malaysia.

ABSTRACT

The aim of this research is to study the impact of statistical moments of probability density function such as mean, standard deviation, skew of R32 flow maldistribution profile on the thermal performance of microchannel heat exchanger under superheat, and sub-cooling effect. A mathematical model was developed in order to analyse the influence of the statistical moments of probability density function of R32 flow maldistribution on the thermal performance of microchannel heat exchanger under superheat and sub-cooling effect. It was found that the high standard deviation and high negative skew of R32 flow maldistribution profile gave a large impact on the D of microchannel heat exchanger and can achieve up to 10%. Moreover, it was found that the heat transfer performance of microchannel heat exchanger dropped significantly when the sub-cool increases. In short, low standard deviation, high positive skew, and superheat of a flow maldistribution profile is preferred in order to minimize the performance deterioration effect. An experiment was set up to verify the mathematical model. The results from the mathematical model agreed well within 10% of the experimental data. A performance deterioration correlation related to refrigerant maldistribution under superheat and sub-cool was developed to provide a faster solution to design an even flow distribution heat exchanger. The proposed correlation in this research offers a quicker and simpler way to study the R32 flow maldistribution problem.

Keywords: Refrigerant maldistribution; microchannel heat exchangers; R32.

INTRODUCTION

Air conditioner contributes a large amount of total energy consumption in buildings as stated in [1]. This paper presents the continuation of the work by Chin and Raghavan [2]. Previous paper studied the impact of the moments of probability density function of air flow maldistribution on the heat transfer performance of a fin tube heat exchanger [3]. It was recommended that mean, standard deviation, and skew should be optimized in the effort of improving the thermal performance of the heat exchanger. Mao et al. [4] found that air flow maldistribution affects the deterioration of condensation capacity and refrigerant pressure drop which are 6% and 34%, respectively. However, they did not analyse the impact of refrigerant flow maldistribution. In the present research, focus is to analyse the impact of refrigerant maldistribution profile in terms of mean, standard

deviation, skew, sub-cool, and superheat on the heating capacity degradation of the heat exchanger under superheat and sub-cooling effect. Nowadays, most designers are having difficulties in designing an energy efficient air conditioner, especially in optimisation of heat exchanger performance. This is due to most of the heat exchangers are facing flow maldistribution problem while a comprehensive mathematical model which can describe flow maldistribution problem is yet to remain a challenge in air-conditioning field. Ablanque et al. [1] also stated that maldistribution situation is particularly unfavourable for two-phase flows due to the possiblility of uneven phase split at each junction of the dividing manifold.

This paper studies the refrigerant maldistribution problem in microchannel heat exchanger (MCHX) which is a highly efficient air-cooled heat exchanger Kurnia and Sasmito [5]. Besides that, Kim and Bullard [6] also indicated that the heat transfer rates per unit core volume are 14% to 331% higher for microchannel condensers as compared to conventional finned round-tube condensers. Moreover, MCHX offers other advantages such as space saving and weight and refrigerant charge [7, 8]. Byun and Kim [9] found that R410A maldistribution in MCHX causes the heat transfer performance reduction by 13.4% compared to the even flow distribution. Zou et al. [10] investigated the flow distribution in MCHX with R410A and R134a. The thermal performance degradation due to refrigerant maldistribution which was affected by header geometry and inlet conditions was simulated. The result showed that the thermal performance was reduced by up to 30% for R410A and 5% for R134a, respectively [11]. Moreover, the impact of flow maldistribution became greater in MCHX which has many micro tubes Dang and Teng [12]. This is due to the tubes are small and tends to have a relatively large manufacturing uncertainty [12]. Said et al. [13] indicated that flow maldistribution can be reduced by roughly 7.5 times by using nozzle approach. Cho et al. [14] performed a numerical study on the mass flow distribution in microchannel heat sink while Kærn and Elmegaard [15] developed a mathematical model of a fin-and-tube evaporator in the object-oriented model language and use R410a as a heat transfer medium. However, their mathematical model did not investigate the influence of the statistical moments of probability density on refrigerant (R32) flow maldistribution in MCHX. The impact of R32 on the air-conditioning system should be analysed in the research as refrigerants with global warming potential (GWP) over 150 from 2011 were suspended in the application of new mobile air-conditioners [16]. This is due to the leakage of high GWP refrigerant from air conditioner which tends to increase the concentration of greenhouse gases in the atmosphere, causing the amount of absorbed infrared radiation to increase, and leading to increased atmospheric temperatures and consequent long-term climate changes [17]. Moreover, reduction in greenhouse gas emission has been discussed since the 1990s [18].

In order to have a comprehensive analysis on the thermal performance deterioration due to flow maldistribution, the effects of higher statistical moments should be considered. Fagan [19] had performed a simulation on flow maldistribution and found that flow maldistribution profile with high standard deviations have high thermal performance deterioration. Kondo and Aoki [20] suggested to use the parameter of standard deviation when determining the thermal performance deterioration factor caused by flow maldistribution. Mondt [21] and Shah and London [22] also suggested using statistical moments such as standard deviation to determine the decrease in NTU (number of heat thermal unit) and Nusselt number. Besides that, Kærn et al. [23] conducted several experiments and haveanalysed the fin-tube evaporator coils by manipulating the superheat of the heat exchanger outlet in order to compensate the deteriotation of heat transfer performance due to flow maldistribution. Hence, it is very crucial to include the

effect of superheat and sub-cool in the analysis of refrigerant maldistribution. Ryu and Lee [24] created new friction and Colburn factors for corrugated louvered fins while Villanueva and de Mello [25] generated the pressure drop and heat transfer correlations for one finned plate heat exchanger. To the best knowledge of the author, none of the researchers developed performance deterioration correlation related to refrigerant maldistribution considering superheat and sub-cool effect [26, 27]. In order to design an optimised air-conditioner system, a comprehensive analysis on refrigerant maldistribution is highlighted in order to estimate the performance deterioration of heat exchanger. Due to this, a performance deterioration correlation related to refrigerant maldistribution under superheat and sub-cool can be developed to allow designers to shorten the development time of air-conditioner with optimised heat exchanger.

METHODS AND MATERIALS

In this research, the fin pattern, number of passes and rows, and air temperature and velocity remain constant. Moreover, this research is only valid for condenser. Çakir and Çomakli [28] stated that the condenser is the component which needs to be improved compared to other components such as compressor and evaporator due to its low energy efficiency [28]. Table 1 shows the geometry configuration of condenser.

Table 1. Geometry configuration of MCHX.

Tubes		Fins	
Height	1.3mm	Pitch	1.2mm
Width	16mm	Height	8.2mm
Number of channels	16	Thickness	0.14mm
Number of tubes	10		
Number of passes	1	**Louver**	
Hydraulic diameter	0.83mm	Length	7mm
		Pitch	1.3mm
Condenser		Height	0.5mm
Length	1700mm	Angle	28°C
Height	103.2mm		
Width	16mm		

In this study, the effects of tube-side maldistribution in term of standard deviation, skew, and mean were investigated. Firstly, a flow maldistribution profile which reflected the three statistical moments (mean, standard deviation and skew) was generated. In order to have a better accuracy, the surface area of the MCHX was discretised into meshes as shown in Figure 1. The mesh size was determined by plotting a graph which is shown in Figure 2.

The deterioration factor, *D*, is shown in Eq. (1).

$$D = (Qu - Qm)/Qu \times 100\%$$
(1)

where *Qu* is the heat transfer capacity for uniform refrigerant flow while *Qm* is the heat transfer capacity for non-uniform refrigerant flow.
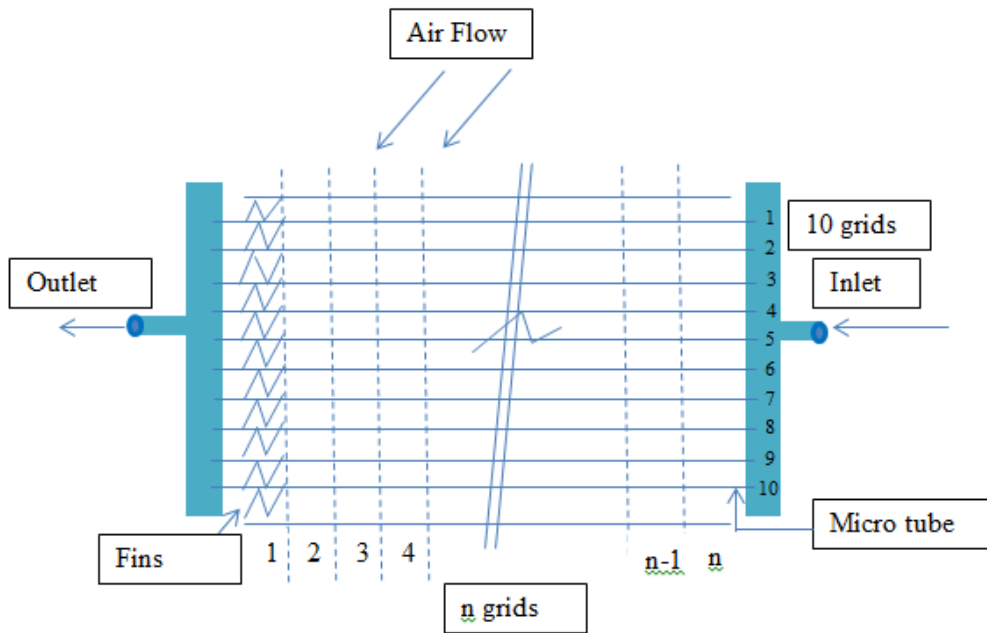
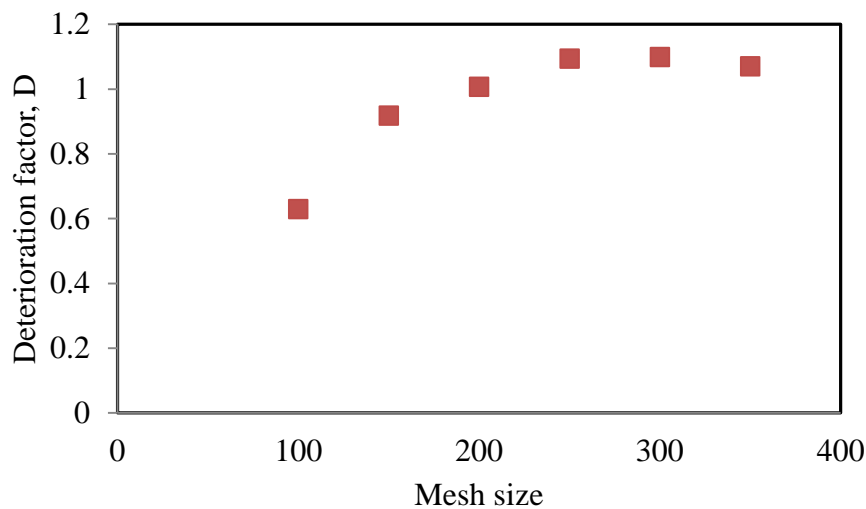Figure 1. Schematic diagram of heat exchanger with 10 x n grids.

Figure 2. Effect of mesh size on deterioration.

From Figure 2, it was found that the degradation of heat transfer performance of MCHX caused by flow maldistribution reached a maximum value and became less susceptible when the mesh size was equivalent to 250. Hence, a mesh size of 250 (10 x 25 grids) was chosen in this mathematical model. In this study, a MCHX with 10 inlets have been chosen to simulate the refrigerant maldistribution profile. Each inlet has its own refrigerant mass flow rate value. The magnitude of these mass flow rates and their required quantities that constitute to the flow distribution profile was generated by continuous probability density functions (PDF) which can be found in Sheskin [29].The local mass flow rate for each mesh was normalised with the mean value in the range of 0.1 to 2.0, at intervals of 0.1.

The heat duty, *q*, for each element was calculated by using the ε-*NTU* method and sum of heat duty for the entire elements yield the total exchanger heat duty. The heat thermal performance of the specific maldistribution profile and uniform distribution profile were calculated. Finally, the thermal deterioration factor of the specific maldistribution profile was calculated. The flow chart of the mathematical model is shown in Figure 3.
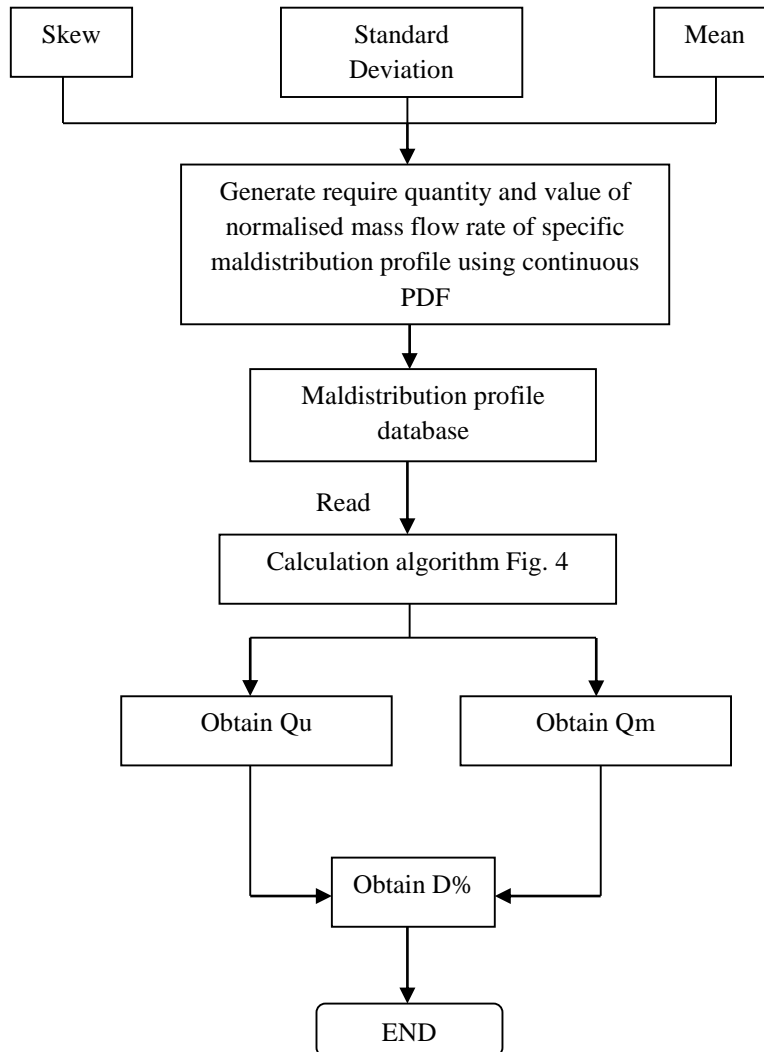
Figure 3. Flow chart of mathematical model.

Heat Transfer Correlation

The air side heat transfer coefficient was calculated using the Colburn factor, *j,* recommended by Chang and Wang [30] for louvered fins. The single-phase refrigerant-side Nusselt number for laminar flow was calculated using the equation provided by Subramaniam [31].For single phase turbulent flow, the Nusselt number can be obtained by using the equation developed by Subramaniam [31]. Huber and Walter [32] claimed that Churchill's equation showed a promising result as its results were within +-10% compared to measured data. Two phase refrigerant side heat transfer correlation was calculated using the correlation developed by Mirza Mohammed Shah PhD [33].
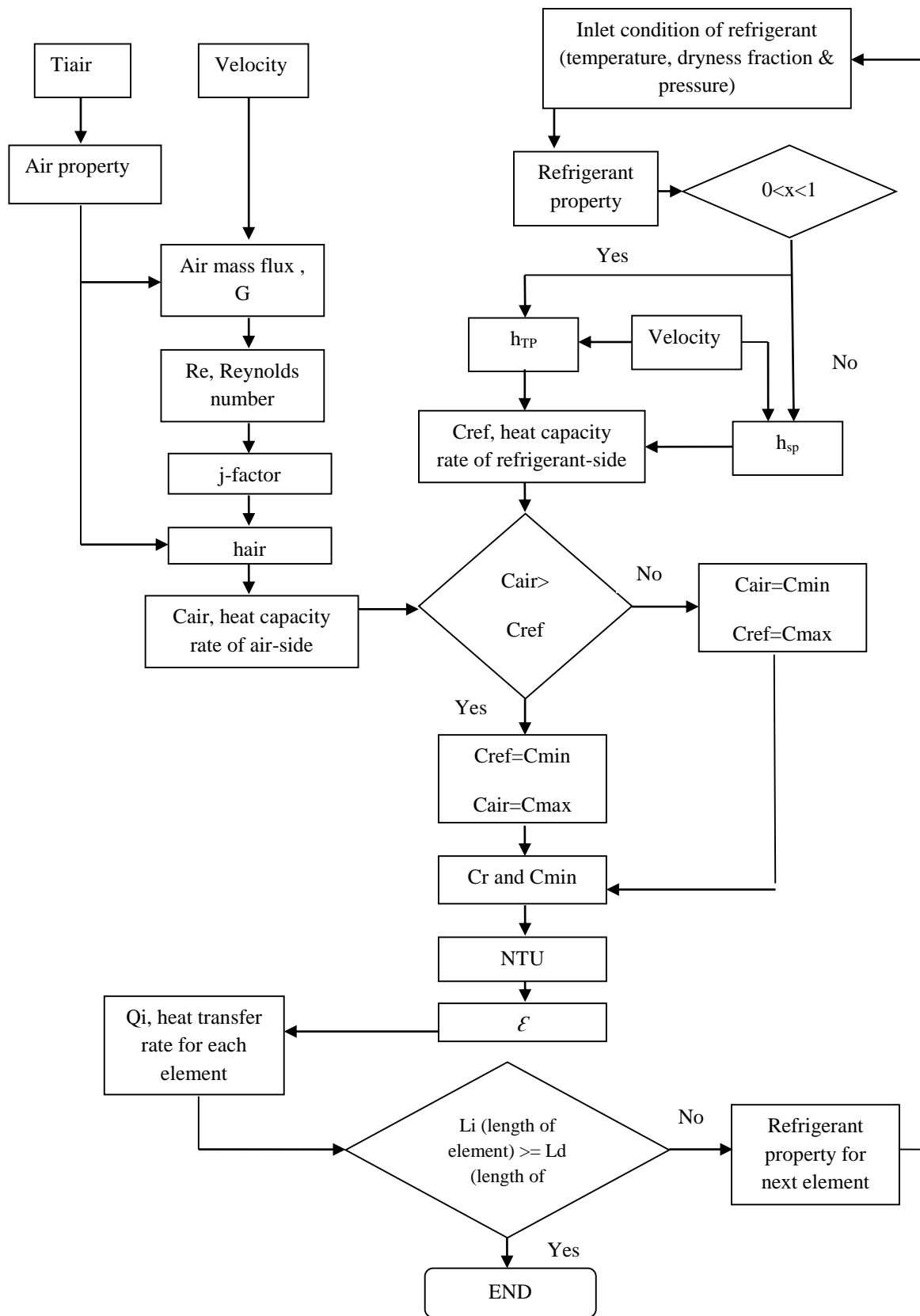
Figure 4. Calculation algorithm to obtain thermal performance.

Pressure Drop Correlation

The refrigerant side single phase pressure drop coefficient was calculated using the single phase pressure drop correlation introduced by Darcy's equation Mott [34]. The friction factor for laminar flow can be calculated by using the equation developed by Yang et al. [35].The friction factor for turbulent flow can be calculated by using the equation developed by Mishima and Hibiki [36]. The refrigerant side two phase pressure drop coefficient was introduced by Mishima and Hibiki [36].

RESULTS AND DISCUSSION

Figure 5 shows the effect of the standard deviation on the D. From the graph, it is shown that higher standard deviation has a major impact on the D. This finding is similar to the result from Chin and Raghavan [37]. Nielsen et al. [38] also stated that the effective thermal performance of heat exchanger decreased as the standard deviation increased. Shojaeefard et al. [39] indicated that flow maldistribution increment (increase of standard deviation from 0.51% to 1.77%) results in about 14% increment in pressure drop and 3.9 % decrement in capacity. The effect is due the larger deviation between the lowest and highest velocities in the flow maldistribution profiles with high standard deviation. Hence, there is a larger net reduction in heat transfer capacity due to the lower heat transfer performance caused by the lower refrigerant velocities which is supported by Chang and Wang [30]. From Figure 5, D is almost equal to zero when the standard deviation approaches 0.1. Besides that, D reaches 3.2% when the standard deviation is high at 0.50.
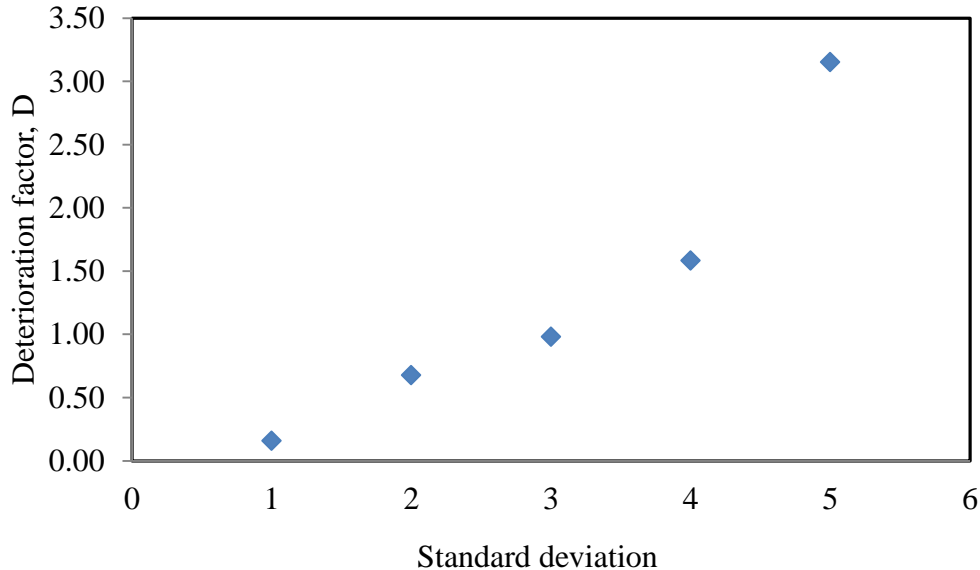

Figure 5. Effect of standard deviation on D.

Figure 6 shows the effect of skew on D. It was found that when the standard deviation is smaller than 0.20, the skew does not have any impact on D. However, it was observed that D varied proportionally with skew when the standard deviations is higher than 0.2. Besides that, it was found that D increases at higher negative skews. The trend is identical to the findings from prior work by Chang and Wang [30] where the flow distribution having a bigger portion of higher velocities neutralise the negative impact of

the lower velocities. Figure 6 also shows that the impact of flow maldistribution on D is very high and reaches up to 10% when the skew is -1. This finding is similar to the research done by Byun and Kim [9].
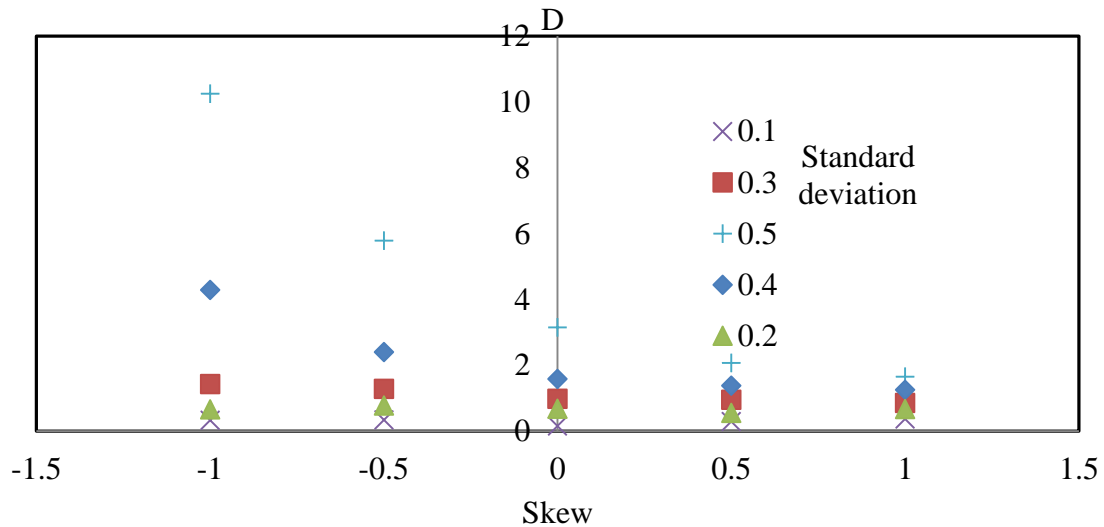

Figure 6. Effect of skew on D.

Figure 7 shows the effect of standard deviation on D with different mean. From the graph, it was observed that lower mass flow rates have a higher impact on the performance deterioration. Besides that, the magnitude of D is greater at a lower mass flow rate and larger standard deviation. The impact of maldistribution was more severe when the mean or mass flow rate is lower where D reaches 4%.
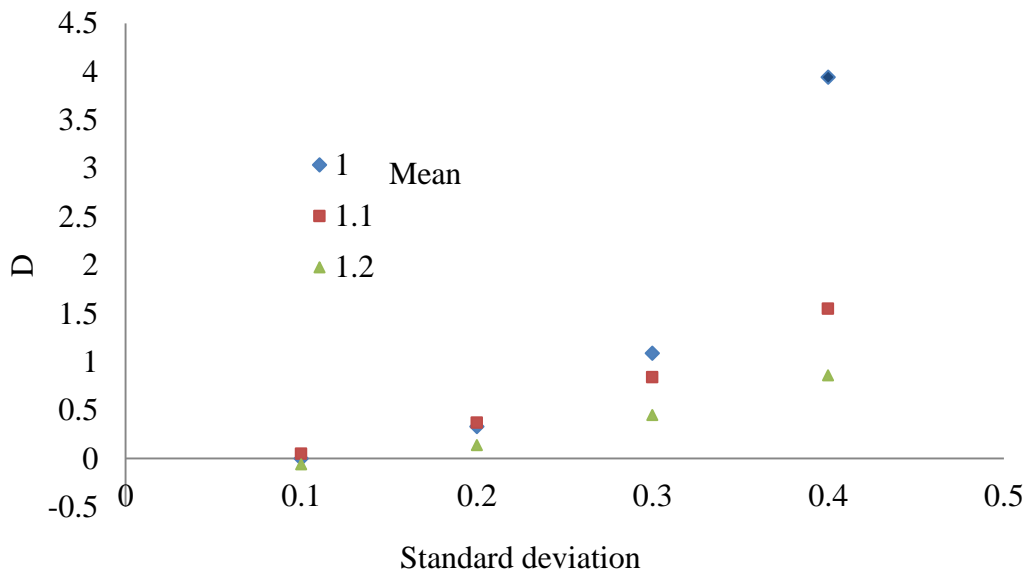

Figure 7. Effect of standard deviation on D with different mean.

Figure 8 shows the effect of mass flow rate on D. From the graph, it is observed that there is very less impact on D when the mass flow rate is more than 60kg/hr. However, D increased significantly when the mass flow rate is less than 60kg/hr where

the sub-cooling region increases. This is due to the sub-cool effect became the dominant factor as the different between ambient and condenser temperature became smaller. The low temperature of refrigerant reduces the difference of temperature between ambient and refrigerant causes the performance of MCHE drops significantly. The maldistribution effect became more sensitive as the larger negative effect of lower velocity or mass flow rate caused by sub-cooling region counteracts the positive effect of higher velocity or mass flow rate. Hence, the sub-cooling effect should be analysed instead of mass flow rate as it dominates the maldistribution effect. The performance deterioration of MCHE reaches at the peak which was around 8% as the sub-cool increased. However, the maldistribution effect was reduced when the sub-cooling region became very large until the MCHE was unable to reject the heat due to the difference of temperature between ambient and refrigerant was very small. Once the temperature of refrigerant at condenser outlet reached ambient temperature, the heat transfer was negligible and approaches zero. The author called the region within this scenario as zero heat transfer region. As the zero heat transfer region of the MCHE increases, the maldistribution effect becomes less susceptible. At this stage, the sub-cool effect or the impact of difference in temperature becomes minimal causing the maldistribution effect to reduce.
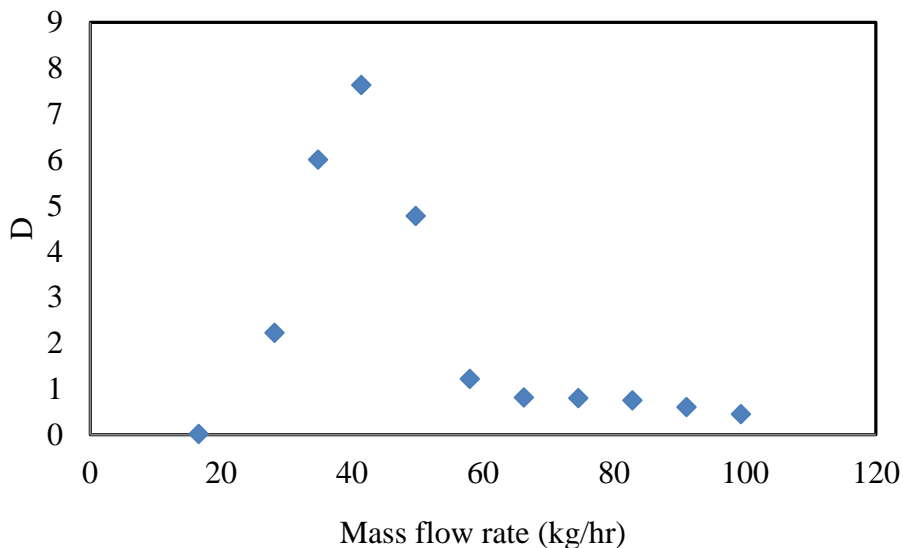

Figure 8. Effect of mass flow rate on the performance deterioration.

Correlation Development
Next, the performance deterioration correlation due to refrigerant maldistribution was developed by determining the relationship between statistical moments and performance deterioration of MCHX. From Figure 8, sub-cool becomes the dominant factor to D compared to mass flow rate. Hence, D versus normalised sub-cool was plotted in Figure 9. In order to improve the accuracy, the author separated the correlation into two regions. Region A is those normalised sub-cool equal and more than 0.43 while region B is those normalised sub-cool less than 0.43. Normalised statistical moments such as normalised skew, standard deviation, and others which were dimensionless parameters were used in the development of performance deterioration correlation.
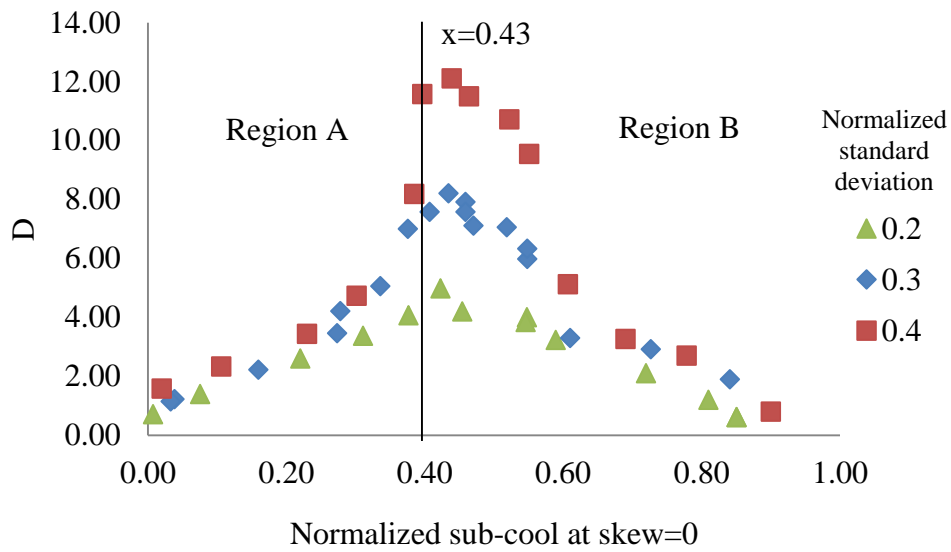
Figure 9. D versus normalised sub-cool at zero skew.

Figure 10 shows D versus the normalised sub-cool at 0.4 of normalised standard deviation. It was found that the different skew had different value of normalised sub-cool at the peak of D. Higher skew had the peak of deterioration at high normalised sub-cool. This is due to the higher skew has large portion of high velocity causes the impact of sub-cool or difference of temperature slower to react on D. However, D increases and reaches the peak as the mass flow rate decreases. Hence, the author used a new parameter which was normalised sub-cool at zero skew in the performance deterioration correlation due to refrigerant maldistribution.
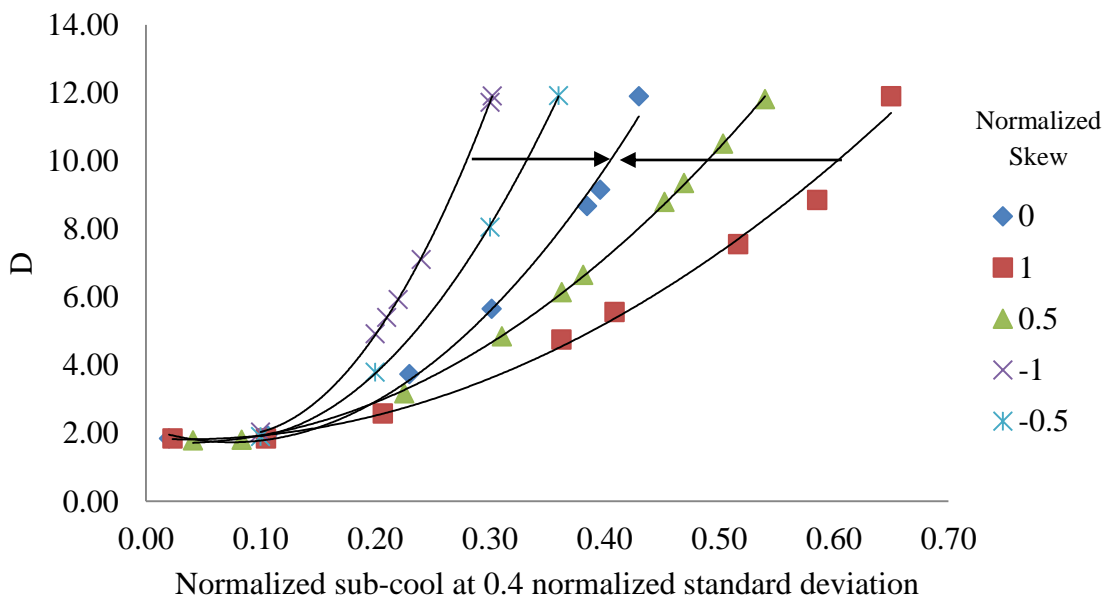

Figure 10. D versus normalised sub-cool at 0.4 normalised standard deviation.

The equation of performance deterioration correlation due to refrigerant flow maldistribution was obtained by applying the observed trends in the previous sections which is shown in Eq. (2).

$$D = (a\sigma'^2 + b\sigma')(c\dot{s}'^2_{0\gamma'} + d\dot{s}'_{0\gamma'} + e) \tag{2}$$

where σ' is normalised standard deviation, $\dot{s}'_{0\gamma'}$ is normalised sub-cool at zero skew, while a, b, c, d and e are constants.

The constants were then solved by non-linear regression analysis. The constants were then calculated by using the Datafit software [40] and the final performance deterioration correlation due to R32 refrigerant flow maldistribution under superheat and sub-cool is shown as below:

in Region A ($\dot{s}'_{0\gamma'} < 0.43$),

$$D = (1.35\sigma'^2 + 2.71\sigma')(55.29\dot{s}'^2_{0\gamma'} + 6.9\dot{s}'_{0\gamma'} + 1.54) \tag{3}$$

$$\dot{s}'_{0\gamma'} = \dot{s}' - (0.99\dot{s}'^2 + 0.23\dot{s}')(-0.22\gamma'^2 + 0.61\gamma') \tag{4}$$

in Region B ($\dot{s}'_{0\gamma'} >= 0.43$),

$$D = (7.02\sigma'^2 + 4.15\sigma')(12.33\dot{s}'^2_{0\gamma'} - 25.02\dot{s}'_{0\gamma'} + 12.84) \tag{5}$$

$$\dot{s}'_{0\gamma'} = \dot{s}' - (0.14\dot{s}'^2 - 0.73\dot{s}' + 0.56)(0.5\gamma'^2 + 0.83\gamma') \tag{6}$$

$$\dot{s}' = \frac{s}{(T_{sat} - T_{ambient})} \tag{7}$$

γ' is normalised skew, s is the average subcool of every circuit, T_{sat} is the saturation temperature of condenser, $T_{ambient}$ is the ambient temperature, ṡ' is normalised sub-cool.

The proposed correlations in this research is able to analyse the maldistribution problem where the designers of HVAC (heating, ventilation, and air conditioning) system only need to insert the value of statistical moments and sub-cool into the proposed equation for a fast estimate of the deterioration factor. Hence, the development of HVAC system is quicker. Moreover, the designers are able to solve the refrigerant maldistribution easily and without using trial and error method.

Measurement of Mass Flow Rate for Each Circuit
The mass flow rate for each circuit can be obtained by using the formula which was suggested by the author. Eq. (8) shows the calculation of the mass flow rate while Eq. (9) shows the calculation of the normalised mass flow rate.

$$\dot{m}_i = \frac{c \times A_i \times \Delta hair_i}{\Delta href_i} \tag{8}$$

where $\dot{m}_i$ is the mass flow rate for each circuit, c is the constant value, Δhref is the difference in enthalpy for refrigerant-side (kJ/kg), Δhair is the difference in enthalpy for air-side (kJ/kg), and A_i is the surface area of each circuits.

$$\text{Normalised mass flow rate, } u' = \frac{\dot{m}_i}{\mu} \text{ (c is eliminated in this equation)} \qquad (9)$$

where μ is the normalised mean of the mass flow rate for each circuit

From the above equation, the surface area, and difference in enthalpy for both air and refrigerant of each circuit are needed to calculate the normalised mass flow rate of each circuit. It is required to measure the pressure of inlet, outlet and temperature inlet and outlet for each circuit to obtain the difference in enthalpy for refrigerant side. The entering air-side temperature for all circuit is same due to even air flow distribution. Next, the leaving temperature for each circuit is required to obtain the difference in enthalpy for air side.

Experiment Verification
An experiment was set-up to verify the mathematical model which was developed by the author. Figure 11 shows the schematic diagram of the test rig. The indoor room temperature was maintained at 27°C while the outdoor temperature was maintained at 35°C. The indoor humidity was maintained at 47% RH (Relative Humidity) while the outdoor humidity was not controlled. This was because the outdoor humidity will not affect the data as the condenser is unable remove the moisture of the room. The inlet and outlet dry-bulb (DB) and wet-bulb (WB) were measured by RTD (Resistance Temperature Detector) sensors. The wet bulb of air leaving temperature was not measured due constant humidity ration for entering and leaving condition. The specific volume of air was obtained by measuring the Dry Bulb and Wet Bulb of condenser inlet condition. The MCHE or condenser was connected to a duct. The duct was made of polyurethane slab and sealed with adhesive cloth tape to ensure no air leakage. The length of duct was around three meter to ensure the air flow entering the duct is even. The air flow rate was measured by drawing the air through the MCHX into a nozzle chamber. Finally, the heating capacity for air is calculated by using the formula which is shown in below:

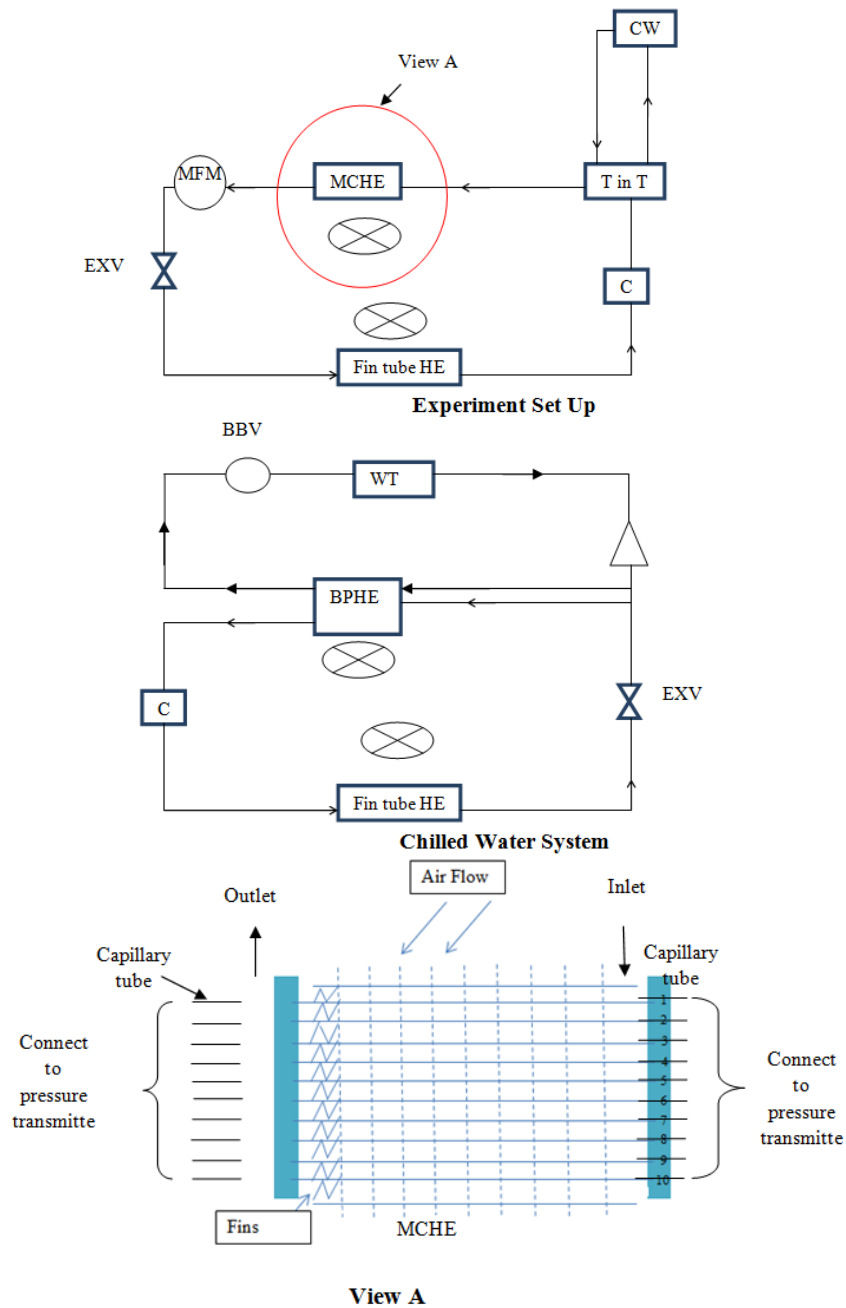$$Q, \text{capacity} = \dot{V} \times 1/\upsilon \times \Delta\text{hair (air side)} \qquad (10)$$

where $\dot{V}$ is the volume flow rate of air (m3/s), $1/\upsilon$ is the specific volume of air (m3/kg) and Δhair is the difference in enthalpy for air side (kJ/kg).

Then, a mass flow meter (MFM) was put at the condenser outlet along the connecting pipe to measure the mass flow rate of refrigerant system. The refrigerant enthalpy leaving and entering the condenser was determined by measuring the condenser inlet and outlet pressure and the respective condenser inlet and outlet temperature. Next, the heating capacity for refrigerant for each circuit was calculated by using the formula which is shown in below:

$$Q, \text{capacity} = \dot{m} \times \Delta\text{href (refrigerant side)} \qquad (11)$$

where $\dot{m}$ is mass flow rate (kg/s) while Δhref is the difference in enthalpy for refrigerant-side (kJ/kg).

Experiment Set Up

Chilled Water System

View A

	Chilled Water		
CW	System	C	Compressor
MFM	Mass Flow Meter	WT	Water Tank
BPHE	Braze Plate Heat Exchanger	Fin tube HE	Indoor Heat Exchanger
MCHE	Micro Channel Heat Exchanger	EXV	Electronic Valve control
T in T	Tube in tube	BBV	Brass Ball Valve
△	Water Pump	⊗	Fan

Figure 11. Experiment set up.

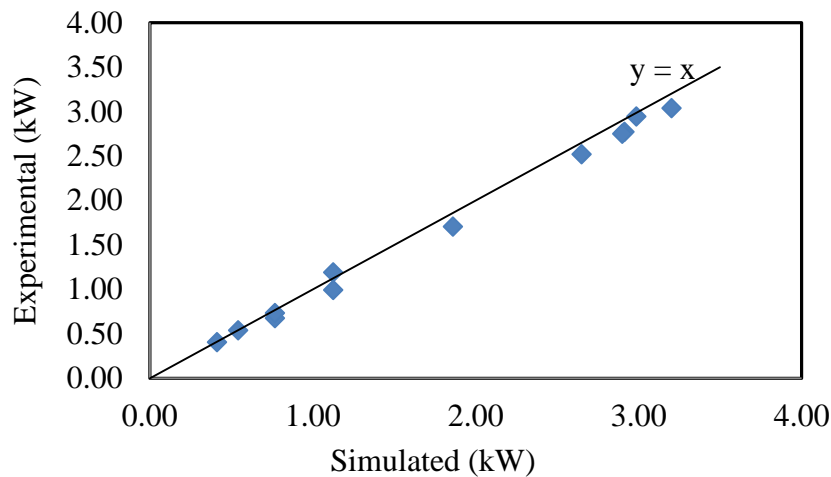Figure 12. Simulated versus experimental result.

Table 2. Simulated versus experimental result.

Mass flow rate (kg/hr)	Experiment capacity (kW)	Simulated capacity (kW)	Sub-cool (°C)	Superheat (°C)	Normalised mean	Normalised skew	Normalised standard deviation
14.19	0.41	0.41	4.5	30.21	1	1.00	0.20
18.97	0.54	0.54	3.5	26.12	1	0.90	0.30
16.53	0.77	0.68	0.76	19.6	1	-0.68	0.35
20.56	0.77	0.73	0.89	28.2	1	1.30	0.30
30.7	1.13	1.19	1.01	20.6	1	0.90	0.15
23.52	1.13	0.99	1.03	27.54	1	1.70	0.20
26.83	1.86	1.7	2.8	28.7	1	-0.20	0.10
37.66	2.65	2.52	3.2	17.2	1	-0.40	0.10
41.2	2.91	2.77	3.6	16.5	1	0.50	0.10
38.81	2.9	2.75	3.7	30	1	0.68	0.10
41.09	2.99	2.94	4.3	26.5	1	0.95	0.10
43.05	3.2	3.04	4.6	25.3	1	1.00	0.10

The air side and refrigerant side capacity must agree well within 6% which is suggested by Handbook [41]. Next, the opening pulse of electronic valve control (EXV) was adjusted in order to get the heating capacity for different mass flow rates. Besides that, the opening of Brass Ball Valve (BBV) was adjusted in order to control different sub-cool and superheat value of MCHE. Twelve data were selected and compared with the simulation result from the mathematical model developed by the author. Figure 12 shows the simulated results versus the experimental results. From the result, it was found that most of the simulated data are within 10% of the experimental data. Only two points of the simulated data fells above +-10%. It was observed that those points have sub-cool value less than 2°C. According to the Ref. [42], the measurement of capacity is valid if the sub-cool value is more than 2°C. When the value of sub-cool is less than 2°C, the

measurement of total mass flow rate becomes inaccurate. The refrigerant flow through mass flow rate meter (MFM) must be fully in liquid form to ensure the measurement of mass flow rate is accurate. Hence, it is suggested to have high sub-cool value in order to ensure that the refrigerant is fully in liquid form when it passes through the MFM.

CONCLUSIONS

It was observed that flow distribution profile with high standard deviation and high negative skew gives a large impact on D of MCHX. The D can be up to 10%. Moreover, it was found that the heat transfer performance of MCHX drops significantly when the sub-cool is high. The impact of refrigerant maldistribution becomes more severe when some of the circuits are in sub-cooling region while others are in saturated region. This was due to the lower heat transfer performance arising from the smaller different between ambient and condenser temperature. Hence, the impact of maldistribution became greater and D increases. Furthermore, it was found that the superheat do not have much impact on the performance deterioration and the difference of performance deterioration factor between 24°C and 4°C superheat was only 0.1%. Additionally, a distribution profile with low standard deviation, high positive skew, high superheat, and low sub-cool is preferred in order to minimise the deterioration effect. Finally, a performance deterioration correlation related to refrigerant maldistribution under superheat and sub-cool was developed to improve the process of developing new HVAC system in term of speed and cost.

ACKNOWLEDGEMENTS

REFERENCES

[1]   Ablanque N, Oliet C, Rigola J, Perez-Segarra C, Oliva A. Two-phase flow distribution in multiple parallel tubes. International Journal of Thermal Sciences. 2010;49:909-21.

[2]   Chin WM, Raghavan VR. The influence of the moments of probability density function for flow maldistribution on the thermal performance of a fin-tube heat exchanger. International Journal of Thermal Sciences. 2011;50:1942-53.

[3]   Tang SH, Chng MH, Chin WM. A review of refrigerant maldistribution. International Journal of Automotive and Mechanical Engineering. 2014;10:1935-44.

[4]   Mao J, Chen H, Jia H, Wang Y, Hu H. Effect of air-side flow maldistribution on thermal–hydraulic performance of the multi-louvered fin and tube heat exchanger. International Journal of Thermal Sciences. 2013;73:46-57.

[5]   Kurnia J, Sasmito A. Heat transfer performance of non-circular coiled tubes-research summary, challenges and directions. International Journal of Automotive and Mechanical Engineering. 2016;13:3710-27.

[6]   Kim M-H, Bullard CW. Performance evaluation of a window room air conditioner with microchannel condensers. Transactions-American Society of Mechanical Engineers Journal of Energy Resources Technology. 2002;124:47-55.

[7] Gupta M, Kasana K, Vasudevan R. Heat transfer augmentation in a plate-fin heat exchanger using a rectangular winglet. Heat Transfer—Asian Research. 2010;39:590-610.

[8] Shojaeefard MH, Nourbakhsh SD, Zare J. An investigation of the effects of geometry design on refrigerant flow mal-distribution in parallel flow condenser using a hybrid method of finite element approach and CFD simulation. Applied Thermal Engineering. 2017;112:431-49.

[9] Byun H, Kim N. Refrigerant distribution in a parallel flow heat exchanger having vertical headers and heated horizontal tubes. Experimental Thermal and Fluid Science. 2011;35:920-32.

[10] Zou Y, Tuo H, Hrnjak PS. Modeling refrigerant maldistribution in microchannel heat exchangers with vertical headers based on experimentally developed distribution results. Applied Thermal Engineering. 2014;64:172-81.

[11] Nielsen KK, Engelbrecht K, Christensen D, Jensen JB, Smith A, Bahl C. Degradation of the performance of microchannel heat exchangers due to flow maldistribution. Applied Thermal Engineering. 2012;40:236-47.

[12] Dang T, Teng Jt. Influence of flow arrangement on the performance of an aluminium microchannel heat exchanger. AIP Conference Proceedings. 2010. p. 576-90.

[13] Said S, Ben-Mansour R, Habib M, Siddiqui M. Reducing the flow mal-distribution in a heat exchanger. Computers & Fluids. 2015;107:1-10.

[14] Cho ES, Choi JW, Yoon JS, Kim MS. Modeling and simulation on the mass flow distribution in microchannel heat sinks with non-uniform heat flux conditions. International Journal of Heat and Mass Transfer. 2010;53:1341-8.

[15] Kærn MR, Elmegaard B. Analysis of refrigerant mal-distribution: In fin-and-tube evaporators. Danske Køledage. 2009:25-35.

[16] Xu X, Hwang Y, Radermacher R. Performance comparison of r410a and r32 in vapor injection cycles. International Journal of Refrigeration. 2013;36:892-903.

[17] Bolaji B, Huan Z. Ozone depletion and global warming: Case for the use of natural refrigerant–a review. Renewable and Sustainable Energy Reviews. 2013;18:49-54.

[18] Yusof T, Anuar S, Ibrahim H. A review of ground heat exchanger for cooling application in the malaysian climate. Journal of Mechanical Engineering and Sciences. 2015:1426-39.

[19] Fagan T. The effects of air flow maldistributions on air-to-refrigerant heat exchanger performance. ASHRAE Transactions. 1980;86:699-713.

[20] Kondo F, Aoki Y. Prediction method on effect of thermal performance of heat exchanger due to non-uniform air flow distribution. SAE Technical Paper; 1985.

[21] Mondt J. Effects of nonuniform passages on deepfold heat exchanger performance. ASME Journal of Engineering for Power. 1977;99:657-63.

[22] Shah R, London A. Effects of nonuniform passages on compact heat exchanger performance. Journal of Engineering for Power. 1980;102:653-9.

[23] Kærn MR, Brix W, Elmegaard B, Larsen LFS. Compensation of flow maldistribution in fin-and-tube evaporators for residential air-conditioning. International Journal of Refrigeration. 2011;34:1230-7.

[24] Ryu K, Lee K-S. Generalized heat-transfer and fluid-flow correlations for corrugated louvered fins. International Journal of Heat and Mass Transfer. 2015;83:604-12.

[25]   Villanueva HHS, de Mello PEB. Heat transfer and pressure drop correlations for finned plate ceramic heat exchangers. Energy. 2015;88:118-25.

[26]   Kumar M, Bhutani V, Khatak P. Research progresses and future directions on pool boiling heat transfer. Journal of mechanical Engineering and Sciences. 2015; 9:1538-55.

[27]   Çomaklı K, UğurÇakır, Şahin E, Kuş AÇ. Energetic and exergetic comparison of air to air and air to water heat pumps according to evaporator conditions. International Journal of Automotive and Mechanical Engineering. 2013;8:1108-20.

[28]   Çakir U, Çomakli K. Determining the working conditions of heat pump components according to running modes. International Journal of Automotive and Mechanical Engineering. 2014; 9:1511-24.

[29]   Sheskin DJ. Handbook of parametric and nonparametric statistical procedures: crc Press; 2003.

[30]   Chang Y-J, Wang C-C. A generalized heat transfer correlation for iouver fin geometry. International Journal of Heat and Mass Transfer. 1997;40:533-44.

[31]   Subramaniam V. Design of air-cooled microchannel condensers for mal-distributed air flow conditions: Georgia Institute of Technology; 2004.

[32]   Huber D, Walter H. Forced convection heat transfer in the transition region between laminar and turbulent flow for a vertical circular tube. International Conference on Fluid Mechanics and Heat & Mass Transfer2010. p. 2010-24.07.

[33]   Mirza Mohammed Shah PhD P. General correlation for heat transfer during condensation in plain tubes: Further development and verification. ASHRAE Transactions. 2013;119:3.

[34]   Mott RL. Applied strength of materials: CRC Press; 2007.

[35]   Yang C-Y, Chen C-W, Lin T-Y, Kandlikar SG. Heat transfer and friction characteristics of air flow in microtubes. Experimental Thermal and Fluid Science. 2012;37:12-8.

[36]   Mishima K, Hibiki T. Some characteristics of air-water two-phase flow in small diameter vertical tubes. International Journal of Multiphase Flow. 1996;22:703-12.

[37]   Chin WM, Raghavan VR. On the adverse influence of higher statistical moments of flow maldistribution on the performance of a heat exchanger. International Journal of Thermal Sciences. 2011;50:581-91.

[38]   Nielsen KK, Engelbrecht K, Bahl CR. The influence of flow maldistribution on the performance of inhomogeneous parallel plate heat exchangers. International Journal of Heat and Mass Transfer. 2013;60:432-9.

[39]   Shojaeefard MH, Zare J, Nourbakhsh SD. Developing a hybrid procedure of one dimensional finite element method and cfd simulation for modeling refrigerant flow mal-distribution in parallel flow condenser. International Journal of Refrigeration. 2017;73:39-53.

[40]   DataFit, Version 9.0. Oakdale Engineering, Oakdale, Pennsylvania, USA, 2010. Retrieved from http://oakaleengr.com.

[41]   Handbook AF. American society of heating, refrigerating and air-conditioning engineers. Inc: Atlanta, GA, USA. 2009.

[42]   ISO 5151. Non-ducted air conditioners and heat pumps – Testing and rating for performance. Geneva, Switzerland: ISO/IEC; 2010.

NOMENCLATURE

T   temperature (°C)
NTU   number of transfer unit (-)
C   heat capacity rate (WK^{-1})
D   deterioration factor (%)
E   expectation function (-)
h   heat transfer coefficient ($Wm^{-2}K^{-1}$)
Q   heat exchanger heating capacity (W)
PDF   probability density function
L   length
Re   Reynolds number
G   air mass flux

Greek letters

ε   heat exchanger effectiveness (-)

Subscripts

i   Index
TP   two phase
SP   single phase
r   Ratio
m   Maldistribution
u   uniform distribution
air   air-side
ref   refrigerant-side
min   Minimum
max   maximum